Lecture 1: Overview

1 Diffusion by discontinous movements

In 1827 Robert Brown, observed that suspended pollen grains are in an uninterrupted and irregular "swarming" motion. Brown was a botanist and at first he believed that only organic materials exhibited this agitation. But very soon he extended his observations to particles of inorganic material, such as a ground-up fragment of the Sphinx. Through the nineteenth century there was a intermittent discussion concerning the cause of this *Brownian motion*, and in 1877 Delsaux suggested that the impact of molecules on a macroscopic particle produces observable displacements. In 1905, after nearly a century of debate, Einstein definitively explained this phenomenon [6, 7].

1.1 Einstein's derivation of the diffusion equation

Our interest here is in Einstein's derivation of the diffusion equation, which is very different from that of Fourier. We consider one-dimensional Brownian motion by projecting the location of the particle onto a straight line which we call the x-axis.

Einstein's assumptions are the following: (i) the particles move independently of one another; (ii) we observe particle positions at time intervals τ which are much greater than the time intervals between molecular collisions. As a result, the motion in one interval is independent of what happened in the previous interval.

In the interval τ each particle has a random displacement Δ along the x-axis. The probability density function (PDF) of Δ is $\phi(\Delta)$. This means that if we observe $N \gg 1$ particles for a time τ then the number of particles which are displaced through a distance which lies between Δ and $\Delta + \mathrm{d}\Delta$ is

$$\mathrm{d}N = N\phi(\Delta)\,\mathrm{d}\Delta. \tag{1}$$

The PDF $\phi(\Delta)$ does not change from interval to interval, and ϕ is symmetric and normalised:

$$\phi(\Delta) = \phi(-\Delta)\,, \qquad \int_{-\infty}^{\infty} \phi(\Delta)\,\mathrm{d}\Delta = 1. \tag{2}$$

The symmetry of ϕ implies that the displacements are unbiased. The average of any function of Δ, $f(\Delta)$, is

$$\bar{f} \equiv \int_{-\infty}^{\infty} f(\Delta)\phi(\Delta)\,\mathrm{d}\Delta\,. \tag{3}$$

In particular, $\overline{\Delta^2}$ is the mean square displacement in a single step.

If the concentration of particles at time t is denoted by $c(x,t)$, then the evolution of c is determined from the *master equation*:

$$c(x, t+\tau) = \int_{-\infty}^{\infty} c(x-\Delta, t)\phi(\Delta)\,\mathrm{d}\Delta\,. \tag{4}$$

The integral over Δ is a sum over the prior locations at time t of the particles that are at x at time $t+\tau$. Thus, the number of particles in the interval $(x-\Delta, x-\Delta+\mathrm{d}\Delta)$ is $c(x-\Delta,t)\mathrm{d}\Delta$ and $\phi(\Delta)$ is the fraction of these particles which jump from $x-\Delta$ onto x.

Figure 1: Simulated Brownian motion using MATLAB; the routine `rand` is used to generate a sequence of 200 random displacements.

If the concentration $c(x,t)$ changes on a length scale which is much greater than the root mean square displacement, then we can approximate the integral equation (4) by the diffusion equation. This assumption that c is slowly varying means that it it is sensible to use a Taylor series expansion

$$c(x,t) + \tau c_t(x,t) \approx \int_{-\infty}^{\infty} \phi(\Delta) \left[c(x,t) - \Delta c_x(x,t) + \frac{\Delta^2}{2} c_{xx}(x,t) \right] \mathrm{d}\Delta. \tag{5}$$

Next, using (2), we reduce (5) to

$$c_t(x,t) \approx D c_{xx}(x,t)\,, \qquad D \equiv \frac{\overline{\Delta^2}}{2\tau}. \tag{6}$$

This is the diffusion equation, and D is the diffusivity.

The greatness of Einstein's contribution to this subject is not the derivation above but rather his formula for the diffusivity of a macroscopic particle

$$D = \frac{RT}{6\pi N_{\mathrm{a}} \nu a}\,, \tag{7}$$

where R is the gas constant, T the absolute temperature, N_{a} the Avogadro number, ν the coefficient of viscosity and a the radius of the particle. Coincidentally, (7) was also discovered in 1905 by William Sutherland in Australia. This relation enabled Perrin to determine Avogadro's number by observing Brownian displacements [7].

The diffusion equation is an approximation of the more exact master equation. As we try to design parameterizations of nonlocal mixing processes, in which scale separation assumptions are shaky, we should pay more attention to this history and consider the possibility of using integral equations such as (4). Notice also that if the Taylor expansion in (5) is continued to higher order then one will usually (i.e. for most kernels ϕ) obtain a hyperdiffusive term such as c_{xxxx}.

1.2 The method of moments

As a check on the derivation of (6), we take a different approach using the method of moments. A *moment* of the concentration is an integral of the form

$$\int_{-\infty}^{\infty} x^n c(x,t)\,\mathrm{d}x. \tag{8}$$

The zeroth moment, $n = 0$ in (8), is the total number of particles:

$$N = \int_{-\infty}^{\infty} c(x,t)\,\mathrm{d}x. \tag{9}$$

The first and second moments can be interpreted as the center of mass and moment of inertia of the concentration profile.

We expect that N is constant, and it is educational to verify this conservation law for both the master equation and the diffusion equation by "taking the zeroth moment". Integrating (4) from $x = -\infty$ to $x = +\infty$, and changing the order of the integrals on the right-hand side gives

$$N(t+\tau) = \int_{-\infty}^{\infty} \mathrm{d}\Delta\, \phi(\Delta) \int_{-\infty}^{\infty} \mathrm{d}x\, c(x-\Delta, t). \tag{10}$$

Changing variables to $x' = x - \Delta$ in the inner integral, and using (2), gives the particle conservation law $N(t+\tau) = N(t)$. The diffusive analog of particle conservation is easily obtained by integrating the diffusion equation (6) from $x = -\infty$ to $x = +\infty$. Provided that Dc_x vanishes at $x = \pm\infty$ (physically, there is no flux of particles from infinity), one immediately finds that $N_t = 0$.

Extending the procedure above to higher moments, we can make a comparison between the exact results for $\int x^n c\,\mathrm{d}x$ and the diffusive approximation of these same integrals. To take the first moment of the diffusion equation, multiply (6) by x and integrate from $x = -\infty$ to $x = +\infty$. Once again, we use integration by parts and assume that terms such as xc_x and c vanish as $x \to \pm\infty$. Thus we find that the center of mass is stationary

$$\frac{\mathrm{d}}{\mathrm{d}t} \int_{-\infty}^{\infty} x c(x,t)\,\mathrm{d}x = 0. \tag{11}$$

The same result can be obtained by taking the first moment of the master equation. The center of mass is stationary because in (2) we assume that the PDF of displacements is symmetric.

Continuing, we come to the second moment. For the diffusion equation we obtain

$$\frac{\mathrm{d}}{\mathrm{d}t}\int_{-\infty}^{\infty} x^2 c\,\mathrm{d}x = 2D\int_{-\infty}^{\infty} c\,\mathrm{d}x = 2DN, \tag{12}$$

where, as before, the terms which fall outside the integration by parts are zero because of the rapid decay of c as $x \to \pm\infty$. The student should show that from the master equation

$$\int_{-\infty}^{\infty} x^2 c(x, t+\tau)\,\mathrm{d}x - \int_{-\infty}^{\infty} x^2 c(x,t)\,\mathrm{d}x = \int_{-\infty}^{\infty} \Delta^2 \phi(\Delta)\,\mathrm{d}\Delta. \tag{13}$$

Recalling the definition of the diffusivity in (6), we see that in the limit $\tau \to 0$ the difference equation in (13) can be approximated by the differential equation in (12).

The law in (12), that the mean square displacement of a cloud of particles grows linearly with time, is often taken to be the defining characteristic of diffusion. As we will see later, there are dispersive processes which have other power-laws, such as $\int x^2 c\,\mathrm{d}x \propto t^{1/2}$. These processes are referred to as "anomalous diffusion".

2 Diffusion by continuous movements

2.1 Lagrangian time series

In 1922 Taylor [11] analyzed the diffusing power of a velocity field. The basic concept here is that of a Lagrangian time series, such as the x-velocity of a tagged fluid particle, $u(t)$, as a function of time. This data is Lagrangian (i.e., following a "float"), *not* Eulerian (i.e, obtained from a "current meter" fixed in space). The velocity time series might look like figure 2. Clearly there is some regularity: evenly spaced maxima and minima are obvious, and we might guess that there is a wave which is producing oscillatory displacements. At the same time, the velocity is not completely predictable, and there is no obvious law by which we can anticipate all details of the future using observations of the past.

The simplest assumption we can make to analyze the process in figure 2 is that the velocity is statistically *stationary*. This means that average properties of the velocity, such as the mean square velocity, are not changing with time. In operational terms, the assumption of stationarity means that if we take nonoverlapping and well-separated subsamples of the time series in figure 2 then the statistical properties of the subsamples are identical.

If the time series is long enough we can chop it into N chunks, each of length T. We define an ensemble average by considering each of the N chunks as a single realization of a random process. This procedure introduces the additional assumptions that there is a decorrelation time $\tau \ll T$, and that time averages are equivalent to ensemble averages. Thinking of dispersion, Taylor imagined that each chunk was an independent particle, labeled $n = 1, 2, ..., N$, executing continuous movements. "Continuous" in this context means that the velocity of particle n, $u_n(t)$, is a relatively smooth function of time, at least in comparison with the jittery motion in figure 1.

We denote the position of particle n by $x_n(t)$, so that if all the particles begin at $x = 0$ then

$$\frac{\mathrm{d}x_n}{\mathrm{d}t} = u_n(t), \qquad \Longrightarrow \qquad x_n(t) = \int_0^t u_n(t')\,\mathrm{d}t'. \tag{14}$$

We use angular brackets $\langle\rangle$ to denote the ensemble average. As an example of this notation, the average velocity of the N particles is

$$\langle u \rangle \equiv \frac{1}{N}\sum_{n=1}^{N} u_n(t). \tag{15}$$

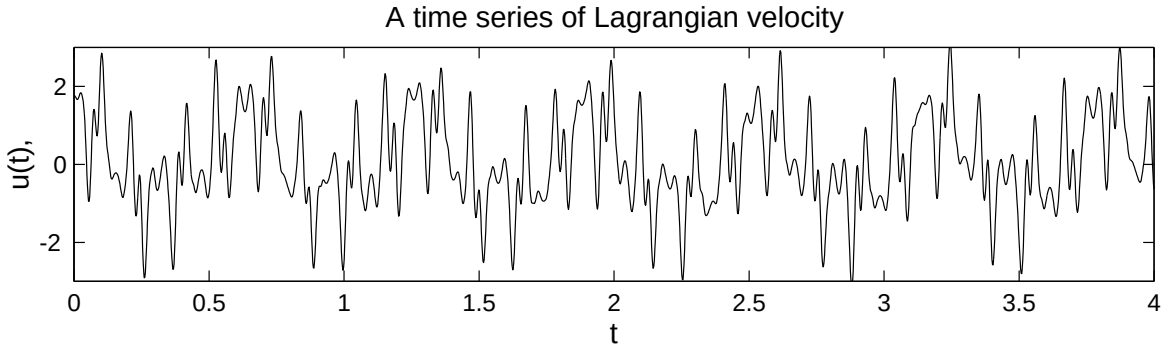

Figure 2: A time series with a spectral peak.

Because of the stationarity assumption, $\langle u \rangle$ is independent of time, and we can refer all displacements relative to the position of the center of mass by writing $x' = x - \langle u \rangle t$ and $u'_n = u_n - \langle u \rangle$. To save decorating all our subsequent x's and u's with primes we now assume that $\langle u \rangle = 0$.

2.2 Taylor's formula

The simplest measure of dispersion about the center of mass is the mean square displacement, $\langle x^2 \rangle$. We can calculate the rate of change of this quantity by first noting that:

$$\frac{\mathrm{d}x_n^2}{\mathrm{d}t} = 2x_n u_n, \qquad \text{and (14)} \Longrightarrow \qquad \frac{\mathrm{d}x_n^2}{\mathrm{d}t} = 2\int_0^t u_n(t)u_n(t')\,\mathrm{d}t'. \tag{16}$$

We now ensemble average (16). Because of stationarity, $\langle u(t)u(t') \rangle$ depends only on the time difference $t - t'$. Thus, we introduce the correlation function

$$\mathcal{C}(t - t') \equiv \langle u(t)u(t') \rangle, \tag{17}$$

and, after a change of variables, write the ensemble average of (16) as

$$\frac{\mathrm{d}\langle x^2 \rangle}{\mathrm{d}t} = 2\int_0^t \mathcal{C}(t')\,\mathrm{d}t'\,. \tag{18}$$

Equation (18) is Taylor's formula, which relates the variance in particle displacement $\langle x^2 \rangle$ to an integral of the Lagrangian velocity autocorrelation function $\mathcal{C}(t)$.

In the simplest situations the correlation function $\mathcal{C}(t)$ decreases rapidly to zero as $t \to \infty$ so that the integral in (18) converges. In this case, the dispersion of the ensemble at large times is characterized by a diffusivity $\langle x^2 \rangle \sim 2Dt$, where the diffusivity D is related to the correlation function by:

$$D = \int_0^\infty \mathcal{C}(t)\,\mathrm{d}t. \tag{19}$$

In statistical physics, (19) is known as the Green-Kubo formula.

Taylor did not claim that turbulent dispersion was governed by the diffusion equation, (6). We will return to this point later. For the moment notice that (6) is an approximation valid only for sufficently long times that the integral in (18) has converged to the constant D. This restriction is related to Einstein's assumption that particle positions are observed at time intervals τ which are much greater than the decorrelation time.

3 Diffusion and anomalous diffusion

In the previous sections we emphasized that the diffusion equation (6) is only valid on times long compared to the decorrelation time τ, and only if the concentration $c(x,t)$ varies on length scales greater than the width of the density $\phi(\Delta)$. These assumptions of scale separation in both time and space are often not satisfied in real flows. Thus, dispersion experiments over the last ten years have revealed behaviours which are much richer than those suggested by the arguments of Einstein and Taylor. Experiments often show that the growth of variance is described by a power law

$$\langle x^2 \rangle \propto t^{\xi}. \tag{20}$$

In some cases $\xi = 1$ (diffusion), but sometimes $\xi \neq 1$, in which case the process is referred to as *anomalous diffusion*.

3.1 Rayleigh-Bénard convection

As an example of hydrodynamic diffusion ($\xi = 1$) and transient subdiffusion ($\xi = 2/3$) we mention the experiments of Solomon and Gollub [9,8] on the dispersion of passive scalar (either methylene blue or uranine dye, or small latex spheres) along a chain of Rayleigh-Bénard convection cells (see figure 3). We refer to the passive scalar generically as "tracer".

Following the experimental procedure in figure 3, suppose that all of the tracer is initially released in a single cell. The main question is: how many cells, $N(t)$, have been invaded by tracer at time t? If this dispersive process is described by diffusion then we expect that $N(t) \propto t^{1/2}$. With certain interesting restrictions, this $t^{1/2}$-law is the experimental result.

The Rayleigh-Bénard flow can be approximately described using a two-dimensional and incompressible velocity field, (u,v), obtained from the streamfunction

$$\psi = k^{-1} A \sin\left[k\left(x + B\sin\omega t\right)\right] W(z)\,, \qquad (u,v) = (-\psi_y, \psi_x)\,. \tag{21}$$

The parameter A controls the amplitude of the flow, $k = 2\pi/\lambda$ is the wavenumber, and $W(z)$ is a function which satisfies the no-slip boundary conditions at $z = 0$ and $z = H$. The term $B\sin\omega t$ is a simple model of the lateral oscillation of the roll pattern which results from an instability which occurs when the convection is driven sufficiently strongly. Because the flow in (21) is simple, highly structured and deterministic, this is not an example of turbulent dispersion. Nonetheless, the experimental results can be summarized using the notion of an *effective diffusivity*.

The Péclet number is

$$P \equiv \frac{A}{k\kappa}, \tag{22}$$

where κ is the molecular diffusivity of the tracer, is a nondimensional parameter which measures the importance of molecular diffusivity to advection. The Péclet number can be considered as the ratio of the time it takes a molecule to orbit around a convection cell to the diffusion time across a cell. In the experiments described here, P is large and molecules make many circuits around a convection cell before Brownian motion jostles them through a distance as large as k^{-1}.

There are two cases which must be carefully distinguished:

Steady rolls The rolls are steady if either $\omega = 0$ or $B = 0$ in (21). In either case, tracer can pass from one roll to a neighbour only via molecular diffusion. But, because molecules are advected through a distance k^{-1}, the dye is transported along the array of cells with an effective diffusivity $D_{\text{eff}} \propto \sqrt{A\kappa/k} \gg \kappa$. Because $D_{\text{eff}} \to 0$ if $\kappa \to 0$, the transport is limited by molecular diffusion.

Unsteady rolls If B and ω are both nonzero then advection (rather than molecular diffusion) can take particles through the time-averaged position of the cell boundaries. In this case, there is the possibility of transport unlimited by weak molecular diffusion.

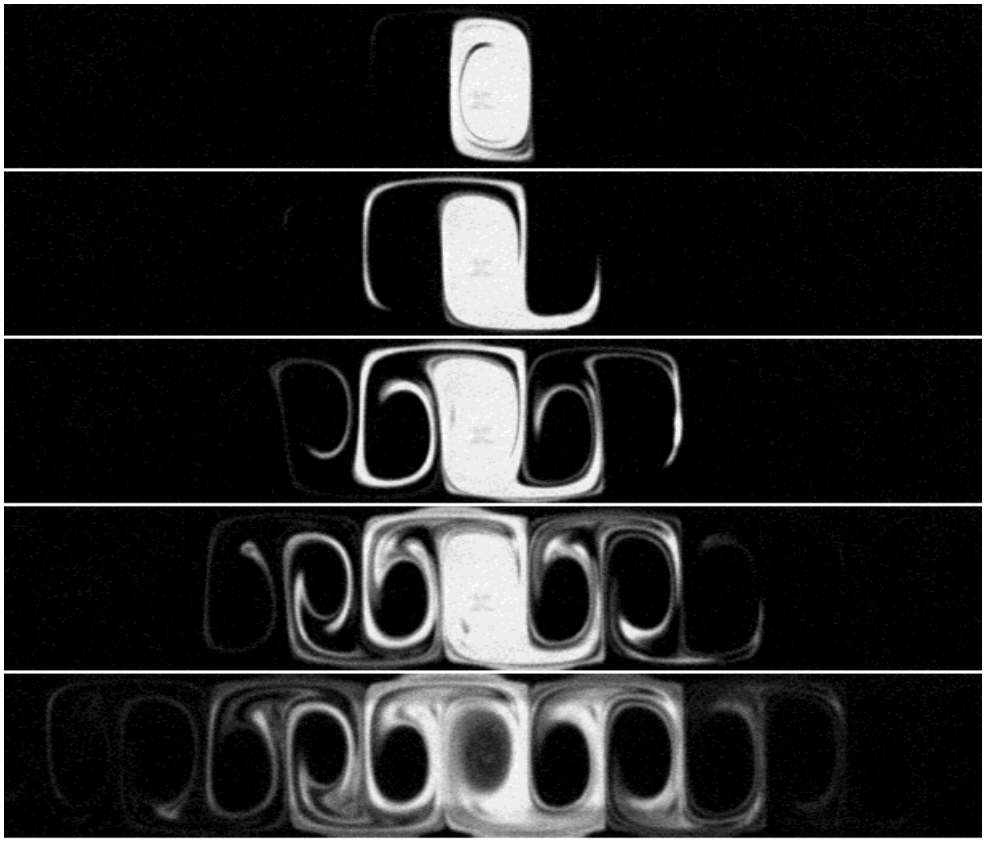

Figure 3: Transport of uranine dye along an array of convection cells with $kB = 0.12$; time (from the top): 1, 2, 4 and 10 periods of oscillation. (Figure courtesy of Tom Solomon [10].)

In the unsteady case, Solomon and Gollub show that trajectories of particles computed with the model streamfunction (21) are similar to the patterns observed experimentally. In both the numerics and the experiments, provided that $\omega B \neq 0$, the transport of particles along the array of cells (in the x–direction) is due to chaotic advection in the neighbourhood of the roll boundaries. This process is strikingly shown in figure 3.

A rough summary of the results is that in both the steady and the unsteady cases the dye spreads via a one-dimensional diffusive process, $\xi = 1$ in (20), with a local effective diffusivity $D_{\rm eff}$. The number of invaded cells is $N(t) \propto \sqrt{D_{\rm eff} t}$. In the unsteady case $D_{\rm eff}$ is independent of the molecular diffusivity κ, while in the steady case $D_{\rm eff} \propto \sqrt{\kappa}$. The effective diffusivity in the unsteady case is enhanced by 1 to 3 orders of magnitude over the effective diffusivity of the steady case (which in turn is much greater than the molecular diffusivity, κ).

The summary in the previous paragraph omits many interesting details. One of the more important caveats is that the effective diffusivity in the *s*teady case only describes the dispersion process at very long times:

$$N(t) \propto t^{1/2} \quad \text{when} \quad t \gg \frac{1}{k^2 \kappa} \,. \tag{23}$$

The time $1/k^2\kappa$ is an estimate of the time taken for molecular diffusion to transport tracer through a distance of order k^{-1}, from the edge of a cell to the center[1]. In this long time limit, the evolution

[1]We assume that the aspect ratio of the cells is of order unity, $kH = O(1)$.

of the tracer is slower than the intracellular diffusion time $1/k^2\kappa$ and consequently the concentration is uniform within each roll. The concentration changes rapidly at diffusive boundary layers (with thickness proportional to $\kappa^{1/2}$) which are located at the roll boundaries. The intercellular flux across these boundary layers is responsible for the spread of the tracer from one roll to the next.

The scenario described above does not have time to become established until $t \gg 1/k^2\kappa$. When $t \ll 1/k^2\kappa$ there is still a significant dispersion of tracer through many cells which is described by the anomalous diffusion law

$$N(t) \propto t^{1/3} \quad \text{when} \quad t \ll \frac{1}{k^2\kappa}\,. \tag{24}$$

The anomalous process above relies on molecular diffusion passing tracer quickly across the cell boundaries before there has been time to reach the center of newly invaded cells [3, 4, 13]. Thus there is a transient regime of subdiffusion which preceeds the final asymptotic diffusive law in (23).

3.2 Anomalous diffusion in two-dimensional turbulence

Cardoso *et al.* [2] conducted an experimental study of dispersion in a quasi-two-dimensional turbulent flow. The experimental apparatus is a shallow pan of fluid, 30cm by 30cm, and 3mm deep. The pan is filled with salty water and flow is driven electromagnetically ($\boldsymbol{E} \times \boldsymbol{B}$ forcing). The forcing is arranged so that the basic flow is a square lattice of 30×30 counter-rotating vortices. This flow is almost two-dimensional because of the large disparity between the horizontal dimensions (30 cm) and the vertical dimension (3 mm).

Although the forcing produces a regular array of vortices, this simple pattern is unstable and a two-dimensional turbulent flow emerges. Visualization of the turbulence, using tracer particles, shows that in the statistically equilibrated state there is a population of vortices whose size is two or three times the injection scale of the forcing. Each vortex emerges, moves, merges with other vortices, and eventually disappears.

Cardoso *et al.* [2] injected dye into this vortex mess and observed the two-dimensional dispersion of the dye in the horizontal plane. To measure the growth of the dye blob, they defined

$$R_m \equiv \int \sqrt{x^2+y^2}\, c(x,y,t)\,\mathrm{d}x\,\mathrm{d}y \Big/ \int c(x,y,t)\,\mathrm{d}x\mathrm{d}y\,, \tag{25}$$

and

$$R_g \equiv \sqrt{\int (x^2+y^2)\, c(x,y,t)\,\mathrm{d}x\,\mathrm{d}y \Big/ \int c(x,y,t)\,\mathrm{d}x\mathrm{d}y}\,. \tag{26}$$

The experimental scaling law is

$$(R_g, R_m) \sim t^{0.32\pm0.04}\,. \tag{27}$$

The exponent $0.32 \neq 1/2$ indicates anomalous diffusion — specifically subdiffusion, because the dispersion is slower than diffusion.

By examining typical particle trajectories, such as the one in figure 4, Cardoso *et al.*explained the subdiffusive growth in terms of an *interrupted random walk*. Consider a random walker who pauses between steps. The length of the pause, τ, is a random variable; in the experiment of Cardoso *et al.*the pause is a trapping event in which a molecule is sequestered in the core of a stationary vortex. If the average duration of a pause is well defined then one can simply use Einstein's formula (6) with τ replaced by the average time between steps. However, if the pausing times are very broadly distributed then the average duration of a pause may be infinite and consequently the dispersion is subdiffusive. We explore this in more details in the next section.

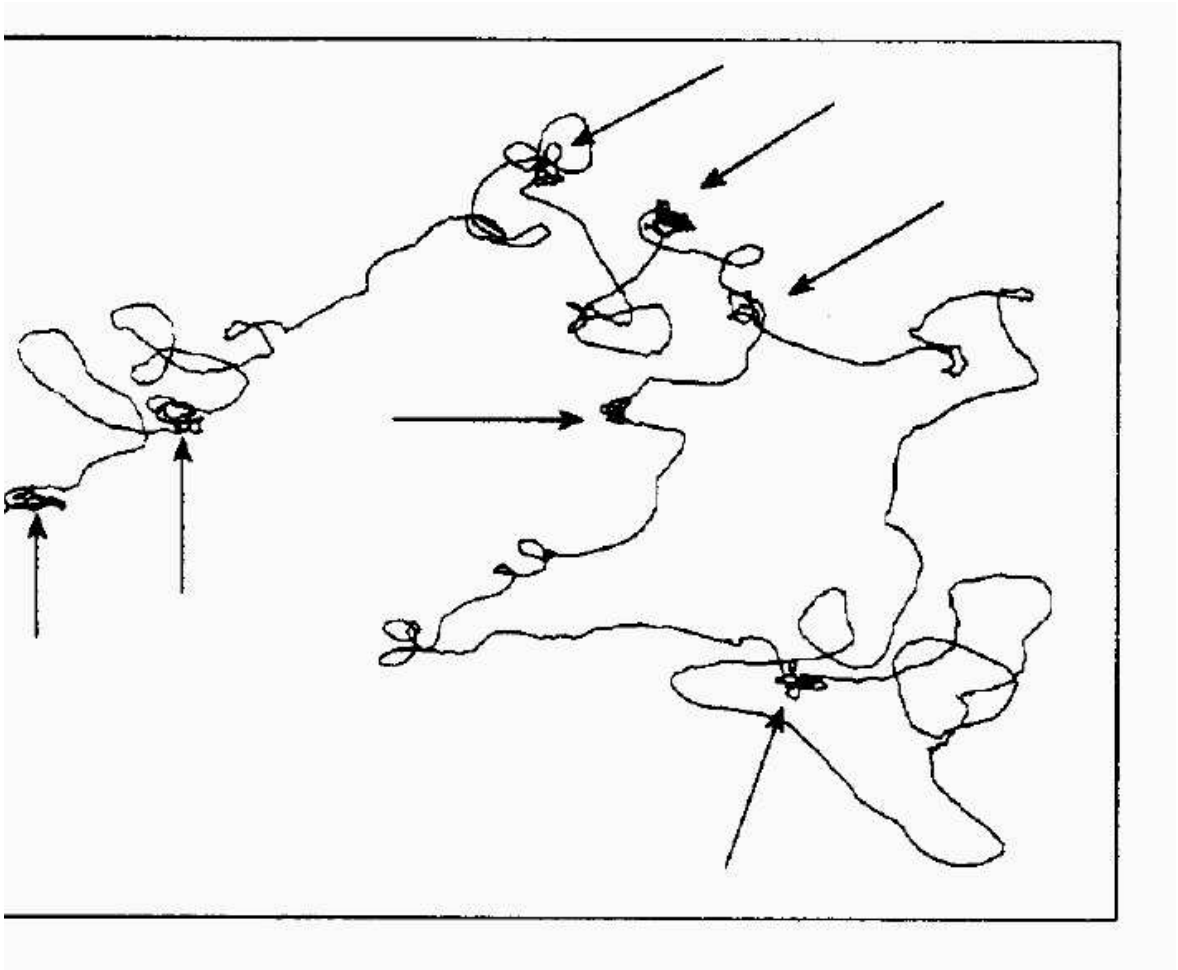

Figure 4: The trajectory of a single particle shows a sequence of long flights interrupted by trapping events in which the particle circles around a vortex. The vortex trapping events are indicated by the arrows. (From Cardoso *et al.* [2])

3.3 Random walk with pauses

Consider a random walk in which the walker pauses for a random time τ between steps. The various τ's have a probability density function $W(\tau)$ (the waiting time PDF). This PDF is normalised,

$$\int_0^\infty W(\tau)\,\mathrm{d}\tau = 1\,, \tag{28}$$

and the average waiting time spent between steps is

$$\bar{\tau} = \int_0^\infty \tau W(\tau)\,\mathrm{d}\tau\,. \tag{29}$$

Motivated by the experiments of Cardoso *et al.*, we entertain the notion that $\bar{\tau}$ is infinite because the integral in (29) diverges. For example, suppose that for large τ, $W(\tau) \sim \tau^{-\mu}$. Then $\bar{\tau} = \infty$ if $\mu \leq 2$.

However, if we only observe a finite number of steps, then we do not sample the entire density $W(\tau)$. Specifically, suppose that after N steps, we have experienced pauses of duration $\tau_1, \tau_2, \ldots, \tau_N$. We want to estimate the likely value of $\tau_{\max}(N) \equiv \max\{\tau_1, \tau_2, \ldots, \tau_N\}$. The quantity $\tau_{\max}(N)$ is useful because we can argue that the structure of $W(\tau)$ for $\tau > \tau_{\max}(N)$ cannot be significant for the displacement after N steps.

To determine $\tau_{\max}(N)$, we turn to probability theory. Consider a random variable θ uniformly distributed in the interval $[0,1]$. That is, the PDF of θ is $P(\theta) = 1$ if $0 < \theta < 1$ and $P(\theta) = 0$ otherwise. Suppose we take N samples, $\theta_1, \cdots, \theta_N$ and define $\theta_{\min}(N) \equiv \min\{\theta_1, \cdots, \theta_N\}$. In this simple case it is plausible that $\theta_{\min} \sim N^{-1}$ as $N \to \infty$.

Now the trick is to use θ to represent τ: we write $\theta = \tau^p$, and adjust p so that the power–law tail of $W(\tau) \sim \tau^{-\mu}$ corresponds to the simple structure of $P(\theta) = 1$. In fact,

$$P(\theta) = W(\tau)\left|\frac{\mathrm{d}\tau}{\mathrm{d}\theta}\right|, \qquad \Longrightarrow \qquad 1 \sim \tau^{1-\mu-p}\,, \tag{30}$$

or $p = 1 - \mu$. Because the minimum value of θ maps to the maximum value of τ, it follows that

$$\tau_{\max}(N) \sim N^{1/(\mu-1)}\,. \tag{31}$$

Now we return to (29) to estimate the effective average pause time after N pauses:

$$\bar{\tau}_{\text{eff}} = \int_0^{\tau_{\max}} \tau W(\tau)\,\mathrm{d}\tau \sim \tau_{\max}^{2-\mu}\,. \tag{32}$$

It is also plausible that the total time t spent on this random walk is given by

$$t \sim N\bar{\tau}_{\text{eff}}\,. \tag{33}$$

Combining (31), (32) and (33) yields the following scaling relationships:

$$N \sim t^{\mu-1}\,, \qquad \bar{\tau}_{\text{eff}} \sim t^{2-\mu}\,, \qquad \tau_{\max} \sim t\,. \tag{34}$$

The final relation is worthy of comment: it implies a form of self-similarity of the random walk.

To conclude, the total displacement of our random walk is proportional to $\sqrt{N}$. But, with the random pauses, the scaling against time has been altered to

$$\text{RMS displacement} \propto \sqrt{N} \sim t^{(\mu-1)/2}\,. \tag{35}$$

This theory can be used to interpret the experiment of Cardoso *et al.*: because the RMS displacement grows as $t^{1/3}$ it follows that $\mu \approx 5/3$. Cardoso *et al.*successfully tested this prediction by measuring the PDF of trapping times inside vortices.

4 Stirring and mixing

4.1 Coffee and cream

Appealing to the everyday experience of mixing cream into coffee, Eckart [5] argued that the homogenization of two fluids occurs in three stages. The distinction between the stages is the value of the concentration gradient averaged over the domain.

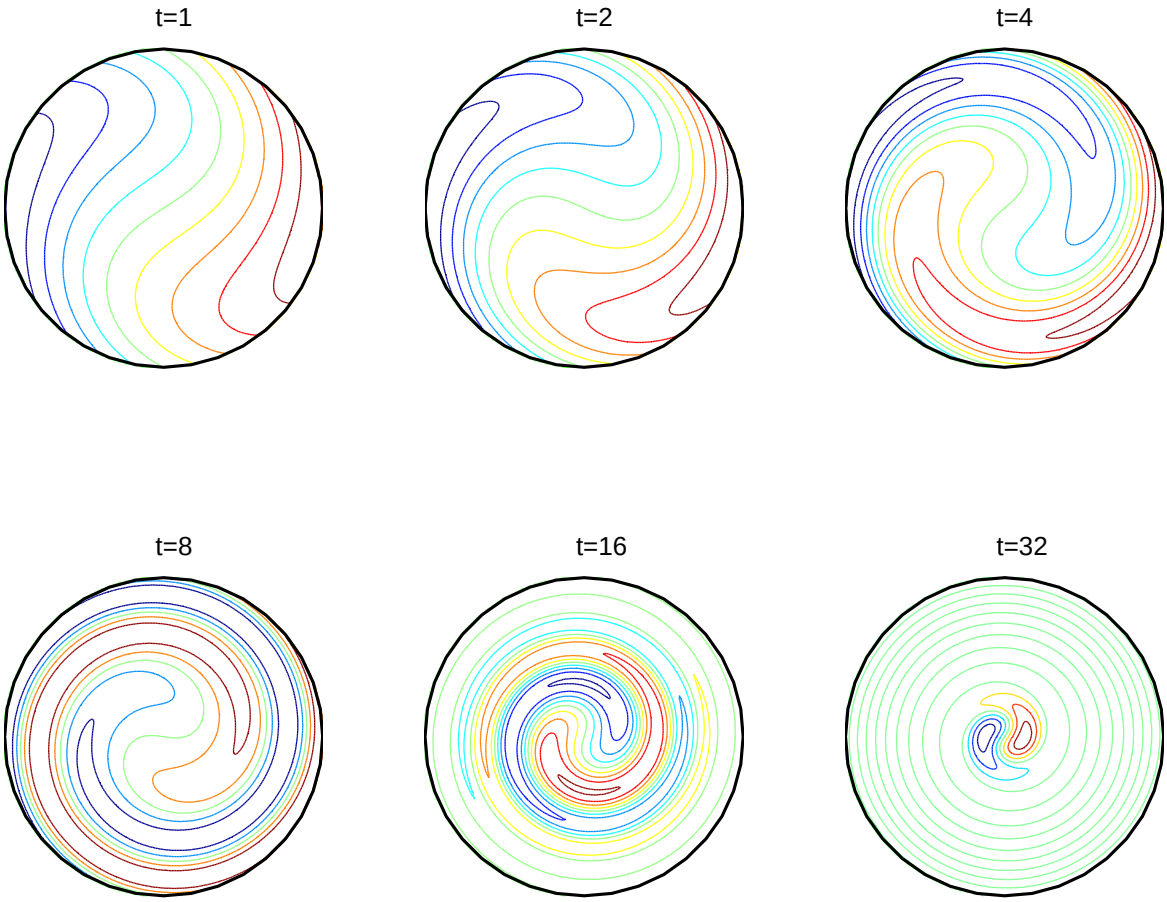

Figure 5: Solution of $c_t + (1-r^2)c_\theta = (8\times 10^{-4})\boldsymbol{\nabla}^2 c$. The initial condition is $c(x,y,0) = x$.

***Initial*:** there are distinct interfaces separating globules of cream and coffee. Within each globule, the concentration of cream is nearly constant and the concentration gradient is close to zero. There is a very large concentration gradient between regions of coffee and cream. But the interfaces between coffee and cream are small in number and not of great area, so the average gradient in the coffee mug is small.

***Stirring*:** the cream is mechanically swirled and folded, and molecular diffusion is unimportant. During this second stage the concentration gradients increase.

***Mixing*:** the gradients suddenly disappear and the fluid becomes homogeneous; molecular diffusion is responsible for the sudden mixing.

In a chemical reaction, molecules of different species must come into contact for the reaction to occur. Thus, when the species are initially separated, the reaction will not begin until the final mixing stage is reached. In this sense there is an important distinction between coarse-grained homogenization, occuring solely as a result of stirring, and mixing at the molecular scale.

To illustrate these concepts figure 5 shows a solution of the advection diffusion equation

$$c_t + (1-r^2)c_\theta = \kappa\boldsymbol{\nabla}^2 c, \qquad c(r,\theta,0) = r\sin\theta \tag{36}$$

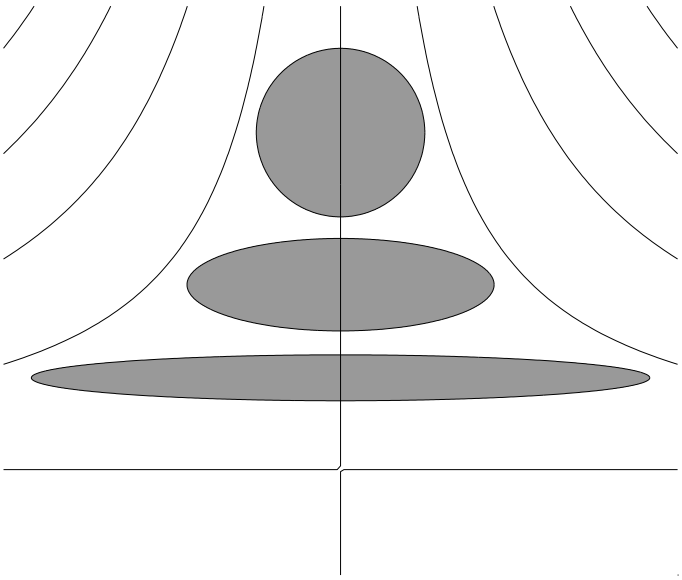

Figure 6: The straining flow described by the streamfunction $\psi = -\alpha xy$. The figure shows how a circular patch of tracer is stretched out along the x–axis by the hyperbolic strain. If $\kappa = 0$ the major axis of the ellipse grows as $\exp(\alpha t)$ and the minor axis reduces as $\exp(-\alpha t)$ so that the area remains constant.

where $\kappa = 8 \times 10^{-4}$. A particle at a distance r from the origin completes a rotation in a time $2\pi/(1 - r^2)$. Thus particles at smaller values of r will overtake particles at larger values of r and so the concentration is twisted into spirals by differential advection (stirring).

The increase in gradient during the stirring phase is evident in the figure. But at approximately $t = 16$, mixing starts to dominate, and diffusion rapidly reduces the average gradient. From the initial condition, an estimate of the time it would take unassisted diffusion to homogenize the fluid is $T_D \sim 1/\kappa = 1250$. It is only through the initial process of stirring that the concentration gradient is amplified or, alternatively, that the spirals are stretched out so that small diffusion homogenizes the tracer at $t = 32 \ll T_D$.

4.2 A straining flow

A simple example of a two-dimensional flow which amplifies concentration gradients is the hyperbolic strain shown in figure 6. The streamfunction is $\psi = -\alpha xy$ and so the advection diffusion equation is

$$c_t + \alpha x c_x - \alpha y c_y = \kappa \boldsymbol{\nabla}^2 c \,. \tag{37}$$

Notice the dimensions here: α^{-1} has dimensions "time" and κ has dimensions (length)^2/(time). From these two quantities we can build a combination with the dimensions of (length):

$$\ell \equiv \sqrt{\frac{\kappa}{\alpha}} \,. \tag{38}$$

The length ℓ will appear prominently in the sequel.

We begin our discussion of hyperbolic strain by obtaining a solution in which c is independent of both x and t. In this special case the solution of (37) is

$$c_y = A \exp\left[-\frac{y^2}{2\ell^2}\right], \quad c(x, \pm\infty, t) = \pm\sqrt{2\pi} A \ell. \tag{39}$$

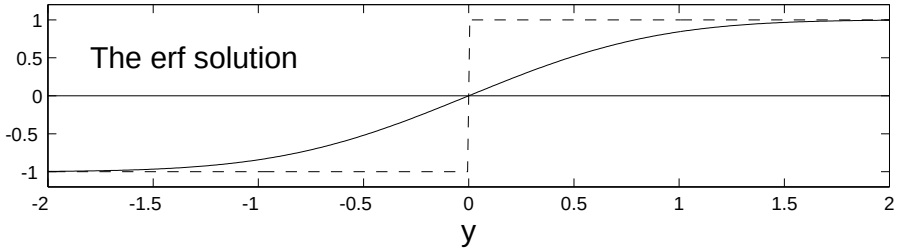

Figure 7: The time independent error function solution to equation (37).

The concentration profile is the error function shown in figure 7. The solution shows the steady state balance between advection and diffusion: with $\sqrt{2\pi}A\ell = 1$, the concentration c changes smoothly between $c = +1$ as $y \to +\infty$ to $c = -1$ as $y \to -\infty$. The transition occurs in a front of width ℓ.

We can give an intuitive discussion of how the steady state profile in figure 7 is established as the solution of an initial value problem. Suppose we had started with the initial condition such as $c(x, y, 0) = \mathrm{sgn}(y)$ in which the transition between $c = -1$ and $c = +1$ occurs in a distance much less than ℓ. Then the discontinuity in c initially diffuses freely, growing like $\sqrt{\kappa t}$. Once the width of the front becomes comparable to ℓ, that is when

$$\sqrt{\kappa t} \sim \ell, \qquad \Longrightarrow \qquad t \sim \alpha^{-1}\,, \tag{40}$$

the spread is arrested and the steady state in figure 7 is established.

On the other hand, we can also consider an initial condition in which the transition between $c = 1$ and $c = -1$ occurs on a scale $L_0 \gg \ell$. In this case the front is initially compressed by the hyperbolic strain so that the width is reduced exponentially, $L = L_0 \exp(-\alpha t)$. Because $L_0 \gg \ell$ the diffusion is unimportant until the exponential reduction in scale reaches ℓ. That is,

$$L_0 e^{-\alpha t} \sim \ell\,, \qquad \Longrightarrow \qquad t \sim \alpha^{-1} \ln(L_0/\ell). \tag{41}$$

These considerations illustrate the fundamental importance of ℓ as the scale on which advection and diffusion come into balance.

4.3 Lagrangian coordinates: a simple example

The hyperbolic strain also provides a painless illustration of some mathematical techniques which can be used in more complicated problems. We begin by considering the solution of (37) with $\kappa = 0$. With no diffusion c is tied to fluid particles. The position of a fluid particle is related to its initial position (a, b), by solving the differential equations

$$(\dot{x}, \dot{y}) = \alpha(x, -y), \qquad \Longrightarrow \qquad (x, y) = \left(e^{\alpha t}a, e^{-\alpha t}b\right). \tag{42}$$

The solution of (37) can now be obtained by arguing that the particle which is at the point (x, y) at time t began at $(a, b) = (\exp(-\alpha t)x, \exp(\alpha t)y)$ at $t = 0$. Because the a particle carries the concentration it follows that the solution of (37) as an initial value problem is

$$c(x, y, t) = c_0\left[\exp(-\alpha t)x, \exp(\alpha t)y\right]\,, \tag{43}$$

where $c_0(x, y)$ is the initial condition. The philosophy of this method is that we care where fluid particles come from, but not where they are going to.

The solution above seems to rely crucially on the restriction that $\kappa = 0$. But now look what happens if we use the Lagrangian coordinates (a, b) in (42) as new independent variables in (37). As

an accounting device, it is comforting to define $\tau = t$ and consider that ∂_τ as the time derivative with (a, b) fixed. Thus the transformation rules are

$$(\partial_x, \partial_y) = \left(\frac{\partial a}{\partial x}, \frac{\partial a}{\partial y}\right)\partial_a + \left(\frac{\partial b}{\partial x}, \frac{\partial b}{\partial y}\right)\partial_b = \left(e^{-\alpha\tau}\partial_a, e^{\alpha\tau}\partial_b\right) . \tag{44}$$

and

$$\partial_t = \frac{\partial\tau}{\partial t}\partial_\tau + \frac{\partial a}{\partial t}\partial_a + \frac{\partial b}{\partial t}\partial_b = \partial_\tau - \alpha a\partial_a + \alpha b\partial_b. \tag{45}$$

The punchline is that

$$\partial_t + \alpha x\partial_x - \alpha y\partial_y = \partial_\tau\,, \tag{46}$$

which shows that the change to a Lagrangian description makes the convective derivative trivial.

Substituting the transformations above into (37) gives:

$$c_t = \kappa e^{-2\alpha t}c_{aa} + \kappa e^{2\alpha t}c_{bb}. \tag{47}$$

Naturally, if $\kappa = 0$, we recover our earlier solution in (43). But even if $\kappa \neq 0$ it is often easier to solve (47) than the Eulerian form in (37). For example, Fourier transforming (47), with $(\partial_a, \partial_b) \to \mathrm{i}(p, q)$, gives a simple ordinary differential equation in time.

It is instructive to use the method above to solve (37) with the initial condition

$$c(x, y, 0) = \delta(x)\delta(y)\,. \tag{48}$$

Physically, this is a spot of dye released in a straining flow. When $\alpha t \ll 1$ the spot spreads diffusively, with a diameter which grows as $\sqrt{\kappa t}$. However when $\alpha t \sim 1$ the diameter of the spot becomes comparable to $\ell \equiv \sqrt{\kappa/\alpha}$, and then the spot stops expanding against the compressive direction of the strain. However the spot continues to stretch along the extensive direction. Thus, when $\alpha t > 1$, the spot becomes a filament with an equilibrium width of order ℓ and an exponentially growing length. These intuitive arguments are supported by the exact solution:

$$c(x, y, t) = \frac{1}{4\pi fg}\exp\left[-\frac{x^2}{4f^2} - \frac{y^2}{4g^2}\right] , \tag{49}$$

where $f(t)$ and $g(t)$ are

$$f^2 \equiv \frac{\kappa}{2\alpha}(e^{2\alpha t} - 1)\,, \qquad g^2 \equiv \frac{\kappa}{2\alpha}\left(1 - e^{-2\alpha t}\right) . \tag{50}$$

Notice that the peak concentration ultimately decreases like $e^{-2\alpha t}$.

4.4 An example of sudden mixing

As a final look at the hyperbolic straining flow, we note that a solution of (37) is

$$c(x, y, t) = A(t)\cos(ke^{-\alpha t}x)\cos(ke^{\alpha t}y), \tag{51}$$

where

$$A(t) = \exp\left[-\ell^2k^2\sinh 2\alpha t\right] . \tag{52}$$

One route to this exact solution is to look for separable solutions of (47), and then transform back to the Eulerian coordinates (e.g., Young, Rhines & Garrett,1982).

The mean value of the square of the concentration gradient varies with time as:

$$\{\boldsymbol{\nabla} c\cdot\boldsymbol{\nabla} c\} = \frac{k^2}{2}\cosh(2\alpha t)\exp\left[-2\ell^2k^2\sinh(2\alpha t)\right] , \tag{53}$$

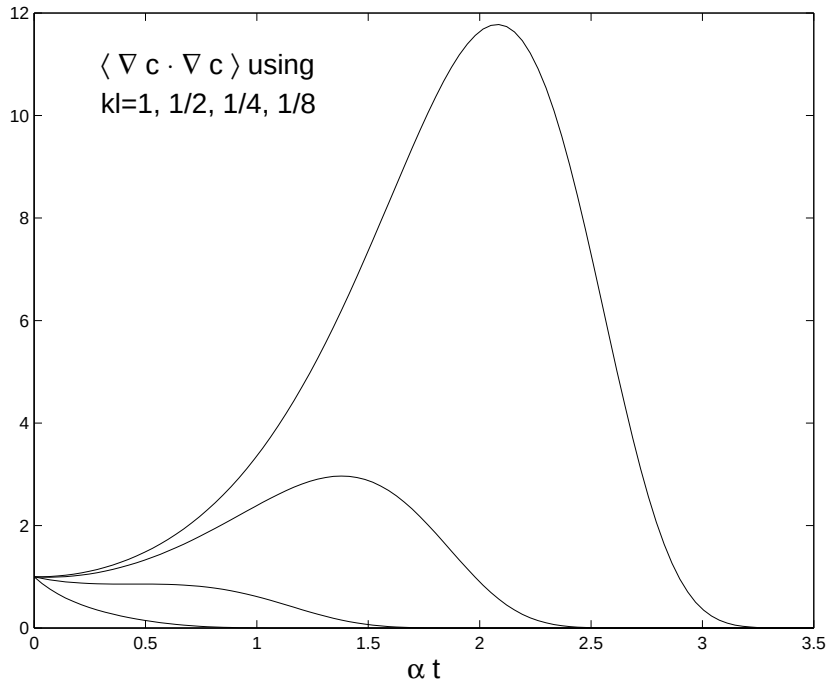

Figure 8: The mean square of the concentration gradient. If $k\ell \ll 1$ then the concentration gradient grows until $t = t_*$ in (54) and then decreases precipitiously. If $k\ell \geq 1/2$ then diffusion always overpowers strain and the mean square gradient decreases monotonically to zero.

where {} denotes an average over a large area. $\{\boldsymbol{\nabla} c \cdot \boldsymbol{\nabla} c\}$ is plotted in figure 8 for various values of $k\ell$. Recalling Eckart's description of stirring as increasing the concentration gradient, and mixing as decreasing the concentration gradient, we can see the transition between the two phases occurs at the peaks of the various curves. If $k\ell \ll 1$, then the time it takes to reach this peak is given by t_*, where

$$\alpha t_* \sim -\ln(k\ell). \tag{54}$$

Once again, this is the time taken for the exponential factor $e^{-\alpha t}$ to reduce initial length of the tracer field, k^{-1}, down to the length ℓ on which strain and diffusion balance.

4.5 A Welander scrapbook

Stirring was beautifully illustrated in a 1955 paper of Welander's [12]. This paper is notable also because of its discussion of the importance of coarse-grained averages. Figures 9, 10 and 11 reproduced from Welander (1955) show that simple velocity fields produce spectacular distortion of passive scalars.

In figures 9, 10 and 11, some dimensions of the scalar blob are stretched out while other dimensions are contracted. Batchelor (1952) [1] argued that in turbulent flows random stretching results in an exponential growth of the separation between two initially adjacent fluid elements. That is, if we consider two material elements separated by a distance s_0 which is much less than the scale of the velocity field, then Batchelor argues that the separation grows as

$$s \sim s_0 e^{\gamma t}\,. \tag{55}$$

The time-scale γ^{-1} is analogous to α^{-1} in (37), though in figures 10 and 11 the exponential straining is driven by a random and unsteady velocity, rather than the simple hyperbolic field in figure 6. Note particularly that the exponential law in (55) is valid until the separation $s(t)$ becomes comparable to the length scale over which the velocity varies.

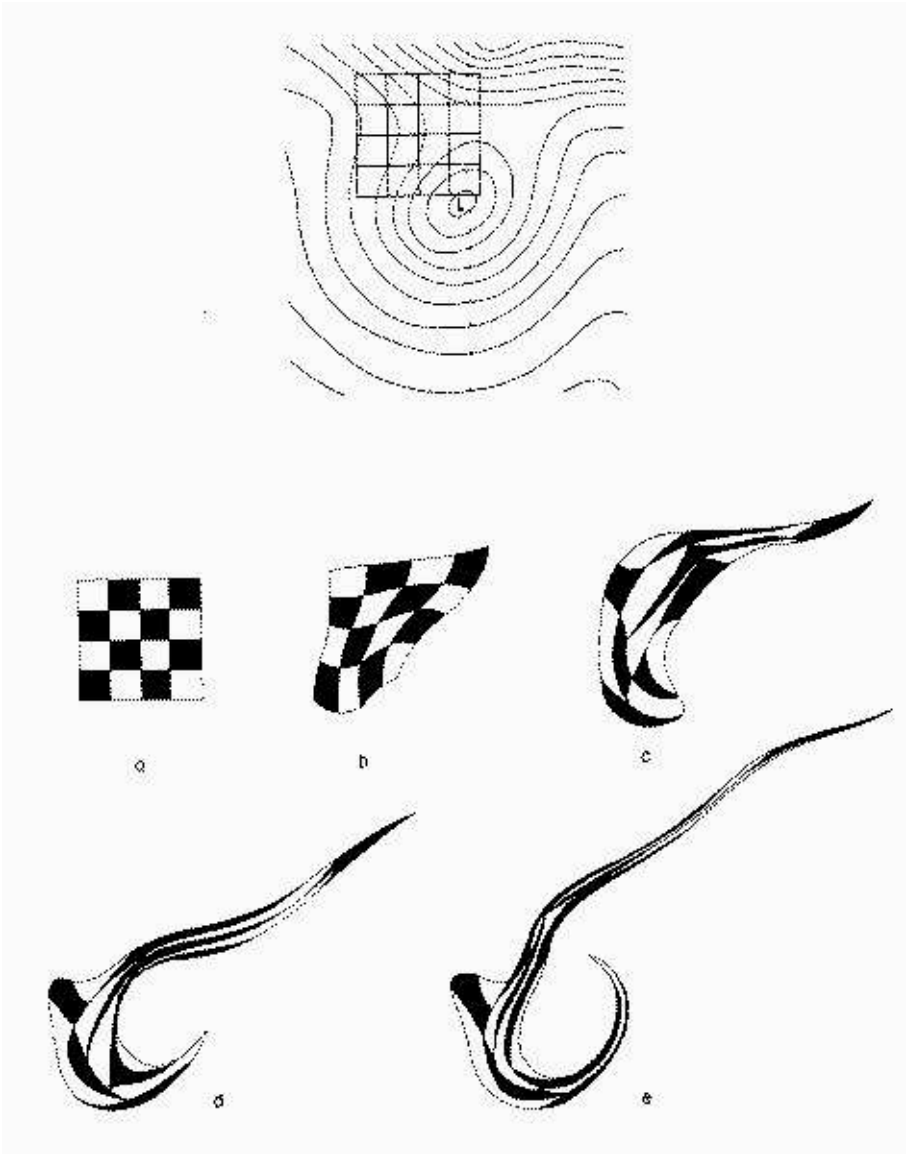

Figure 9: Welander's numerical solution illustrating differential advection by a simple velocity field. A checkerboard pattern is deformed by a quasigeostrophic barotropic solution which models atmospheric flow at the 500mb level. The initial streamline pattern is shown at the top and the subsequent figures are at 6 hours, 12 hours, 24 hours and 36 hours, respectively. Notice that each square of the checkerboard maintains constant area as it deforms.

References

[1] G.K. Batchelor. The effect of turbulence on material lines and surfaces. *Proc. Roy. Soc. London A*, 213:349–366, 1952.

[2] O. Cardoso, B. Gluckmann, O. Parcollet, and P. Tabeling. Dispersion in a quasi-two-dimensional turbulent flow: an experimental study. *Phys. Fluids*, 8(1):209–214, January 1996.

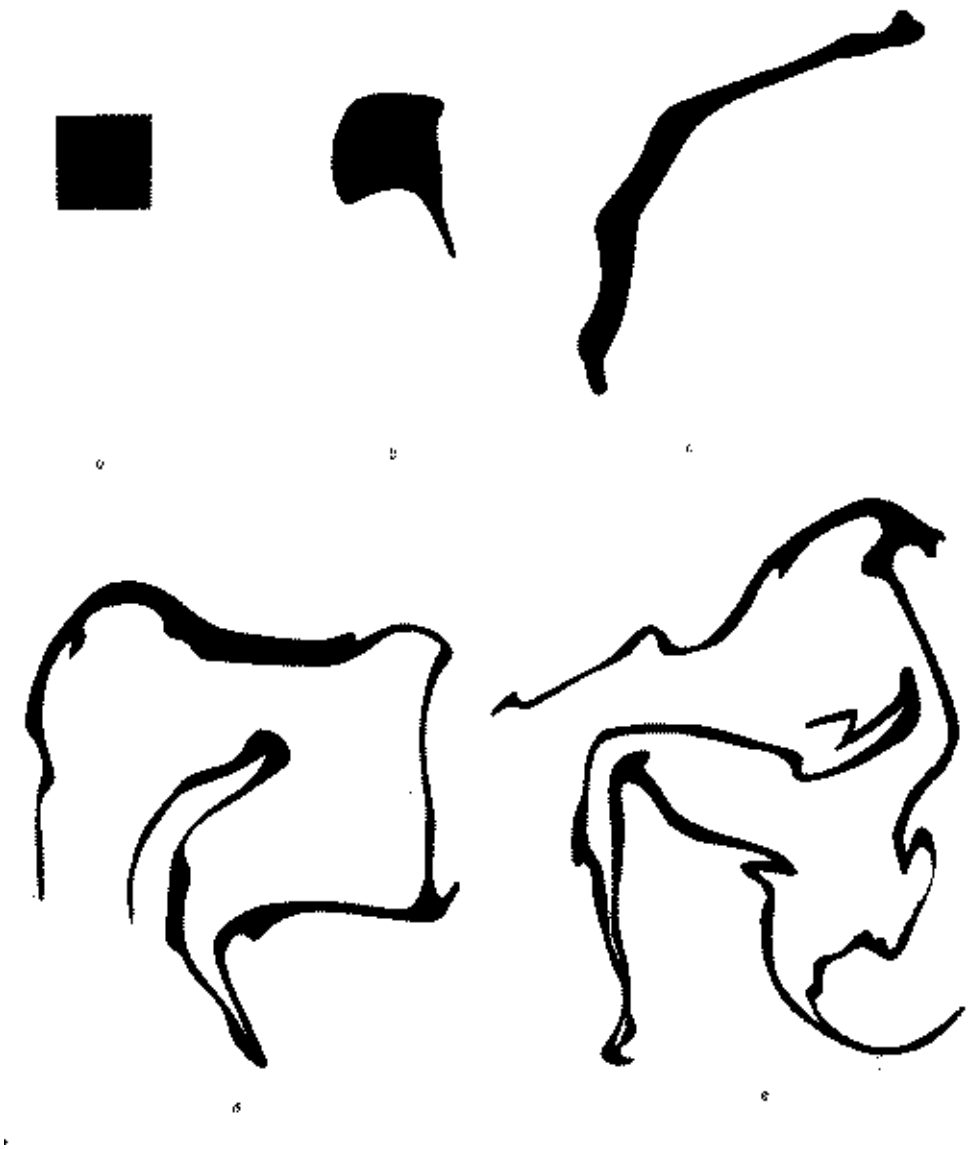

Figure 10: Welander's experimental illustration of the deformation of a small coloured square element of a fluid surface. To suppress three dimensional turbulence, a vessel of water is brought into solid body rotation. A floating film of butanol is divided into square elements by means of a metal grid and one of these square elements is coloured with methyl-red. The solid body rotation is disturbed by stirring the water and the grid is removed.

[3] O. Cardoso and P. Tabeling. Anomalous diffusion in a linear array of vortices. *Europhys. Lett.*, 7(3):225–230, 1988.

[4] O. Cardoso and P. Tabeling. Anomalous diffusion in a linear system of vortices. *Euro. J. Mech. B/Fluids*, 8(6):459–470, 1989.

[5] C. Eckart. An analysis of stirring and mixing processes in incompressible fluids. *J. Mar. Res.*, 7:265–275, January 1948.

Figure 11: Further deformation of the butanol square in figure 10. According to Batchelor [1], the length of the filaments increases exponentially with t.

[6] A. Einstein. *Investigations on the theory of the Brownian Movement.* Dover, New York, 1956.

[7] A. Pais. *'Subtle is the Lord...'.* Oxford University Press, Oxford and New York, 1982.

[8] T.H. Solomon and J.P. Gollub. Chaotic particle transport in time dependent Rayleigh-Bénard convection. *Phys. Rev. A*, 38:6280, 1988.

[9] T.H. Solomon and J.P. Gollub. Passive transport in steady Rayleigh-Bénard convection. *Phys. Fluids A*, 31:1372–???, 1988.

[10] T.H. Solomon, S. Tomas, and J.L. Warner. Chaotic mixing of immiscible impurities in a two-dimensional flow. *Phys. Fluids A*, 10:342–350, 1998.

[11] G.I. Taylor. Diffusion by continuous movements. *Proc. London Math. Soc.*, 20:196–212, 1921.

[12] P. Welander. Studies on the general development of motion in a two-dimensional, ideal fluid. *Tellus*, 7:141–156, 1955.

[13] W.R. Young, A. Pumir, and Y. Pomeau. Anomalous diffusion of tracer in convection rolls. *Phys. Fluids A*, 1:462–469, 1989.

[14] W.R. Young, P.B. Rhines, and C. Garrett. Shear-flow dispersion, internal waves and horizontal mixing in the ocean. *J. Phys. Ocean.*, 12:515–527, 1982.